



Intramolecular photoinduced electron transfer for cations derived from azole-substituted coumarin dyes

Guilford Jones II* and Jennifer Ann C. Jimenez

Department of Chemistry and the Photonics Center, Boston University, Boston, MA 02215, USA

Received 8 September 1999; accepted 24 September 1999

Abstract

The conjugate acids of 7-aminocoumarins that are substituted with benzimidazole or benzothiazole groups display long wavelength absorption and emission associated with low-lying charge transfer states; rapid radiationless deactivation is proposed to proceed via TICT-type intermediates. © 1999 Elsevier Science Ltd. All rights reserved.

Coumarin heterocycles that are substituted in the 7-position with an amine function constitute an important class of fluorescent materials.¹ Their acid-base properties have been infrequently studied, but results show that on protonation at the 7-amine site, the dye chromophore is altered, concomitant with changes in luminescence or lasing properties.² Among the varieties of readily synthesized coumarin dyes of this type, are structures that are substituted in the 3-position with an additional heterocyclic ring. Dyes such as 1–3 remain highly fluorescent and show moderate red shifts due to conjugation of linked aryl groups.^{1,3} We have explored more thoroughly the acid-base properties of these azole-substituted coumarin derivatives, focusing on the accessible conjugate acids that result from the basicity of the imidazole (benzothiazole) ring nitrogen (for benzimidazole, $pK_a=5.48$).⁴ In a recent related study, the conjugate acid form of 3 has been shown to have novel properties on taking up binding sites in zeolite Y.⁵ We find for 1–3 that the monocation derivatives show red-shifted bands that can be associated with an excited charge transfer state (ICT). The quenching of fluorescence can be best understood in terms of discrete intramolecular electron transfer involving coumarin and azole fragments. This mechanism is consistent with formation of an intermediate in which charge is shifted to the coumarin moiety and decay proceeds via a twisted ICT species, reminiscent of the well known TICT states that are widely reported.^{6,7}

Coumarins 1–3 (Eastman Kodak and Acros Organics) were only sparingly soluble in water but dissolved readily in 30% (v/v) ethanol/water. On titration of the dyes in this medium with trifluoroacetic acid (TFA), dramatic spectral changes took place in the form of a red shift of absorption and emission bands with the addition of moderate amounts of acid followed by shifts to the blue on further acidification

* Corresponding author.

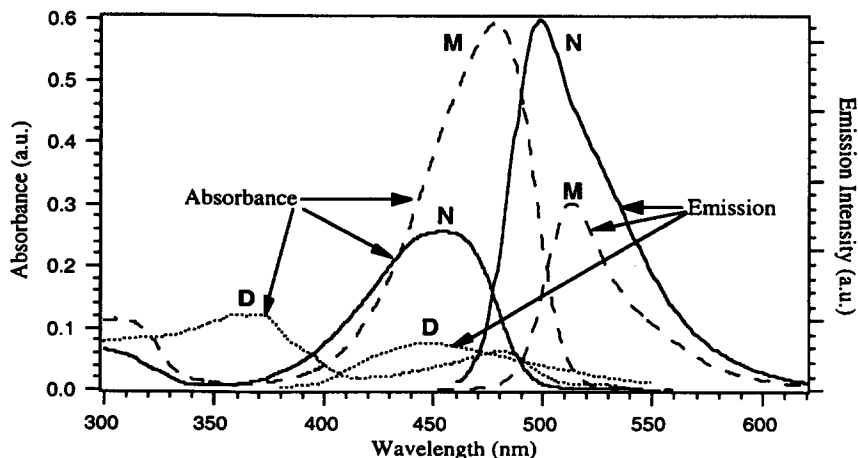
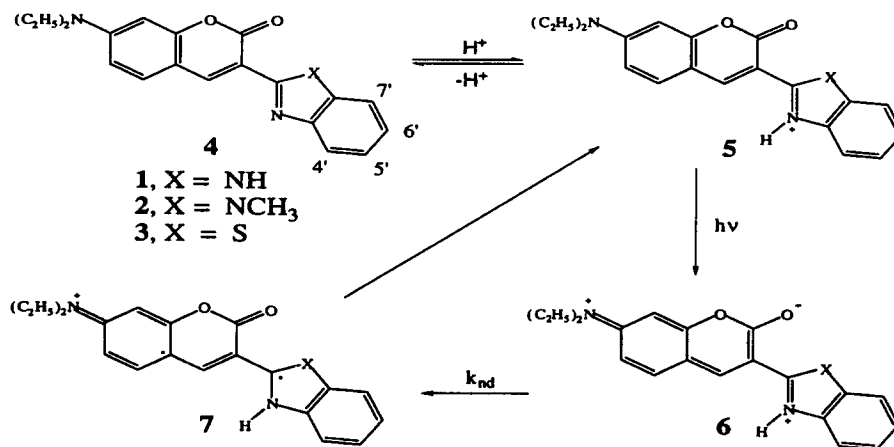


Figure 1. Absorption and emission spectra for coumarin 1 in the neutral (N), monocation (M) and dication (D) forms. 5 μM dye in 30% EtOH/H₂O

(Fig. 1). Assignments regarding sites of protonation can be made from NMR data; for example, proton resonances are shifted downfield most noticeably for theazole substituent (in CDCl₃, $\Delta\delta=0.5$ for proton 7', $\Delta\delta=0.3$ for proton 6') at 0.5 M TFA, as noted previously⁵ for 3. Chemical shifts were further altered with additional acid present (1 M) ($\Delta\delta=0.9$ for the N(CH₂CH₃)₂ substituent). These changes are associated with the expected acid-base equilibria, first involving protonation at azole nitrogen (5) (Scheme 1) with subsequent formation of the dication associated with exocyclic nitrogen protonation for more acidic solutions. The recording of absorption spectra as a function of 'pH'[†] led to nominal pK_a values for 1–3 of 5.0, 4.6, and 0.92, respectively, a trend that is consistent with the higher basicities reported for benzimidazoles versus benzothiazoles.⁴



Scheme 1.

The marked red shift and increased absorptivity of the principal visible band on protonation is consistent with formation of a low lying ICT state in which the charge that is separated, primarily within

[†] Measurements were made using an Orion 420A pH meter fitted with an Ag calomel electrode; pK_as were taken from recorded values of 'pH' for 30% EtOH/H₂O solutions and do not reflect values for pure water solutions.

Table 1
Photophysical properties of coumarin dyes and their monocations^a

	medium	$\lambda_{\text{a}}, \text{nm}$ $\epsilon \times 10^3 (\text{M}^{-1} \text{cm}^{-1})$	$\lambda_{\text{f}}, \text{nm}$	Φ_{fr}	τ, ns	$k_{\text{nd}},$ 10^8 s^{-1}	E_{oo}, eV
1	30% EtOH	454 (91)	498	0.52	2.4	2.0	2.57
	30% EtOH (H ⁺)	479 (119)	513	0.25	0.48	16.	2.48
2	30% EtOH	425 (54)	489	0.25	1.3	5.9	2.70
	30% EtOH (H ⁺)	450 (58)	504	0.13	0.33	12.	2.58
3	30% EtOH	473 (44)	512	0.35	2.1	3.1	2.51
	30% EtOH (H ⁺)	518 (52)	543	0.10	0.41	22.	2.34

^a[dye] = 5 μM in aqueous EtOH, with and without 1.7 M TFA

the coumarin moiety as with most related 7-aminocoumarin derivatives, is further stabilized by the 3-imidazolium substituent. Shown in Scheme 1 are the equilibria that give rise to the monocations, along with a depiction of excitation leading to intramolecular charge transfer (ICT) states **6**. A second protonation at the aniline-type exocyclic nitrogen provides the UV-absorbing dicationic form (not shown), for which the coumarin chromophore has been diminished in both conjugation and CT interaction. Although varying in intensity, each of the protonated forms of **1–3** gives rise to fluorescence that mirrors the absorption features (Fig. 1). The measurement of fluorescence quantum yields[‡] and lifetimes[§] for the neutral and the cationic species was informative in the dissection of competing radiative and non-radiative pathways. Shown in Table 1 are spectral data for **1–3** for both neutral solutions, and acidic media that produce the monocations **5**.

The photophysical data primarily show a reduction in quantum yield and lifetime for emission from **1–3** in acidified media. These features signal an introduction of a non-radiative decay channel, a 'short-circuiting' mechanism that involves forward and reverse electron transfer and the intermediacy of charge-shift species **7**. The latter is of some structural interest in that it incorporates two radical centers, one of which (the benzimidazole) is merostabilized⁸ and another that is stabilized through extensive π -electron conjugation. The legitimacy of this structure can also be evaluated from redox potential data. Protonation of the azole rings for **1–3** results in dramatic enhancement of electron acceptor ability as indicated in reported reduction potentials for 2-arylbenzimidazoles or -benzothiazoles (e.g. $E_{\text{red}} = \text{ca. } -0.7$ and -2.0 V versus SCE, DMF solvent, for protonated forms versus neutral species, respectively). Electron donor capabilities likewise have been reported for the 7-aminocoumarin moiety (E_{ox} (**3**) = 1.02 versus SCE, CH₃CN).⁹ Development of a low lying charge-shift state is then expected (from the redox potential data, at ca. 1.7 eV, an energy below that corresponding to the zero-zero band, E_{oo} , associated with ICT fluorescence, Table 1). This type of charge-shift (cationic) intermediate is similar to those arising from 9-aryl-10-methylacridinium dyes.¹⁰

In order to inspect the aspect of twisting of molecules (cations) about the central bonds that join coumarin and azole halves, MOPAC calculations were conducted to assess barriers to rotation. Computations resulted in the prediction of a minimum energy geometry for **1** in which the angle made by ring planes is 0 and 30°C, respectively, for the neutral and cationic forms (Fig. 2) in the ground state. The nominal

[‡] Quantum yields ($\pm 10\%$) were recorded using coumarin **6**, **7** ($\Phi_{\text{f}} = 0.82$, EtOH) and coumarin **30** ($\Phi_{\text{f}} = 0.80$, EtOH) as references.

[§] Lifetimes ($\pm 10\%$) were measured from single exponential decays obtained using a PTI LaserStrobe fluorimeter.

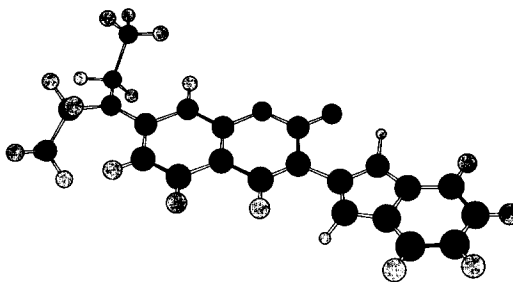


Figure 2. Molecular model for the protonated form of 1

energy barrier for rotation about the biaryl bond, associated with the geometry in which an all-planar arrangement of rings for the cationic form is achieved was 26.7 kcal/mol.

The mechanistic model that is supported in part by the computational results relies on the structural subtlety that is associated with the cationic forms of 1–3; i.e., the requirement for twisting due to non-bonded repulsion of C=O, N–H, and C–H sites. The electronic states that are available to the cation then include an excited ICT state (**6**) largely localized on the coumarin with the azolium 3-substituent. Lying below the ICT species is **7**, the charge shift intermediate that results from electron transfer between heterocyclic rings. The latter would be expected to adopt a highly twisted geometry, conforming to the ‘minimum overlap rule’ that has been noted for numerous intermediates of the TICT variety.^{6,7} Rates for deexcitation of ICT states (**6**→**7**), reflected in the values of non-radiative decay, $k_{nd}=(1-\Phi_f)/\tau_f$ (Table 1) are moderate and remain in a favorable range for fluorescence measurement. An apparent trend in these data is the modest decrease in k_{nd} for coumarin ICT states that have higher energy gaps, E_{00} (Table 1), possibly an indication of ‘inverted region’ behavior for relatively exoenergetic electron transfer.¹¹

In summary, the photophysical properties of heterocycle-substituted 7-aminocoumarins are modified sharply on protonation in mixed aqueous media. Reduced quantum yields and lifetimes of fluorescence for cationic coumarins can be understood in terms of the imposition of a low-lying electron–transfer state, an example of a twisted intramolecular charge transfer (TICT) intermediate. The trends observed provide an array of measurement benchmarks for further use of fluorescence probes of this type^{3,5,7,12} for assessing the local acidity of microenvironments.

Acknowledgements

This work was supported by the US Department of Energy, Division of Basic Energy Sciences.

References

1. (a) Jones II, G. In *Dye Laser Principles with Applications*; Duarte, F. J.; Hillman, L. W., Eds.; Photochemistry of Laser Dyes. Academic Press: New York, 1990; (b) Jones II, G.; Jackson, W. R.; Choi, C. *J. Phys. Chem.* **1985**, *89*, 294.
2. Karandashova, L. A.; Kirpichenok, M. A.; Yufit, D. S.; Struchkov, Y. T.; Grandberg, I. I. *Khim. Geterotsikl. Soedin.* **1990**, *12*, 1610.
3. Nemkovich, N. A.; Baumann, W.; Reis, H.; Zvinevich, Yu. V. *J. Photochem. Photobiol. A: Chem.* **1997**, *109*, 287.
4. Hofmann, K. In *Imidazole and Its Derivatives, Part I*; Interscience Publishers: New York, 1953.
5. Scaiano, J. C.; Corrent, S.; Hahn, P.; Pohlers, G.; Connolly, T. J.; Fornes, V.; Garcia, H. *J. Phys. Chem. B* **1998**, *102*, 5852.
6. Rettig, W. In *Topics in Current Chemistry*; Matlay, J., Ed.; Springer Verlag: Berlin, 1994; Vol 169, p. 253.

7. Jones II, G.; Farahat, M. S. In *Advances in Electron Transfer Chemistry*; Mariano, P. S., Ed.; JAI Press: Greenwich, Connecticut, 1993; Vol. 3, pp. 1–32.
8. Baldock, R. W.; Hudson, P.; Katritzky, A. R.; Soti, F. *J. Chem. Soc., Perkin Trans. 1* **1974**, *12*, 1422.
9. Jones II, G.; Griffin, S. F.; Choi, C.; Bergmark, W. R. *J. Org. Chem.* **1984**, *49*, 2705.
10. (a) Jones II, G.; Farahat, M. S.; Greenfield, S. R.; Gosztola, D. J.; Wasielewski, M. R. *Chem. Phys. Lett.* **1994**, *229*, 40. (b) Jones II, G.; Yan, D.; Greenfield, S. R.; Gosztola, D. J.; Wasielewski, M. R. *J. Phys. Chem.* **1997**, *101*, 4939.
11. Turro, N. J.; Kavarnos, G. *Chem. Rev.* **1986**, *86*, 401.
12. Jones II, G.; Jimenez, J. A. C. *J. Photochem. Photobiol. A: Biol.* submitted.